Assessing light absorption contributions in thin periodically-textured silicon absorbers under oblique illumination

Ahmadpanahi, H.; El Gawhary, O.; Vismara, R.; Isabella, O.; Zeman, M.

DOI
10.1063/1.5090344

Publication date
2019

Document Version
Final published version

Published in
AIP Advances

Assessing light absorption contributions in thin periodically-textured silicon absorbers under oblique illumination

Cite as: AIP Advances **9**, 045001 (2019); https://doi.org/10.1063/1.5090344
Submitted: 26 January 2019 . Accepted: 20 March 2019 . Published Online: 01 April 2019

H. Ahmadpanahi, O. El Gawhary, R. Vismara, O. Isabella, and M.Zeman

Assessing light absorption contributions in thin periodically-textured silicon absorbers under oblique illumination

Cite as: AIP Advances 9, 045001 (2019); doi: 10.1063/1.5090344
Submitted: 26 January 2019 • Accepted: 20 March 2019 •
Published Online: 1 April 2019

H. Ahmadpanahi,[1,a)] O. El Gawhary,[2,3] R. Vismara,[1] O. Isabella,[1] and M.Zeman[1]

AFFILIATIONS

[1] Department of Electrical Sustainable Energy, Delft University of Technology, 2628 CD Delft, The Netherlands
[2] Imaging Physics Department, Delft University of Technology, 2628 CD Delft, Netherlands
[3] VSL, Dutch Metrology Institute, 2629 JA Delft, Netherlands

[a)] S.H.Ahmadpanahi@tudelft.nl

ABSTRACT

Periodic texturing is one of the main techniques to enhance light absorption in thin-film solar cells. The presence of periodicity, such as grating, allows the excitation of guided modes in the structure, thus enhancing absorption. However, grating efficiency in exciting guided modes is highly dependent on the wavelength and incident angle of light. This is relevant especially in solar cells application, where the light source – the sun – is broadband and largely angle-dependent. Nevertheless, most of literature only focuses on the frequency response of periodic texturing, thus neglecting the effect of angular movement of the sun. In this work we use Fourier expansion to calculate the absorption of each type of mode (guided and non-guided) in an absorptive periodic waveguide. The structure is illuminated with TM and TE polarized light and under three different incident angles. Using this method, we are able to calculate the contribution of a guided resonance to total absorption for different angles of incidence. The work here developed and supported by rigorous numerical calculations can be used to better understand light propagation in a periodic waveguide structure, such as thin-film solar cells.

INTRODUCTION

Sun is a broadband and largely angle-dependent light source. Its spectrum consists of a wide range of frequencies from UV to IR.[1] To better exploit the solar spectrum for photovoltaic (PV) energy conversion, enormous efforts are dedicated to multi-junction solar cells,[2–12] spectrum splitting[13–17] and different light trapping schemes,[18] especially focused on the longer wavelength range,[19–28] close to the bad gap of the absorber materials. However, in very few of these studies the angle of incidence is considered to be not perpendicular to the surface of the solar cell.[29–31] Applications such as concentrator photovoltaic and spectrum splitters only work under normal incidence.[32] Therefore, sun tracking systems are implemented to ensure an optimal system performance. On the other hand, in conventional PV installations, where solar cells are mounted in a fixed position, the angle of incidence changes at every moment. This influences light absorption in the solar cell, especially for solar cells endowed with random or periodic texturing. In our previous work, we considered normal incidence in our analysis to distinguish between guided and non-guided absorption resonances in a periodically-textured thin-film solar cell.[33] We note that non-guided modes are also known as leaky modes for which $k_x \leq k_0$, where k_0 is the wave vector in the incident medium. In this contribution, we extend our analysis to the case of oblique incident angles.

A simple way to find the guided modes of a multilayer slab, albeit applicable to (mostly) flat interfaces, is to plot the reflection or transmission coefficients using a Fabry-Perot formula for $0 < k_x < large\ values$ (say, much larger than k_0, where k_0 is computed in the incident medium).[34–36] Then, every time one comes across a resonance for an incident $k_x > k_0$, that resonance corresponds to a guided mode.[37] However, as we focus on textured slabs, we employ instead a Fourier expansion to decompose the electric field inside a periodically textured thin-film solar cell. Then, the

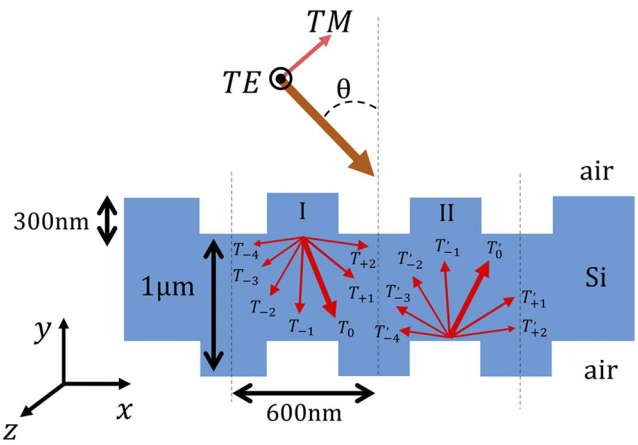

FIG. 1. A 1-μm thick nc-Si:H waveguide, endowed with 1-D front and rear gratings and characterized by a total thickness of 1 μm at every point. The structure is illuminated under an oblique incident angle with TE (electric field parallel with z axis) and TM (electric field perpendicular to z axis) polarizations. Region I and II show light scattering from each interface. T_i and T'_i are the transmission and reflection from the front and rear interfaces, respectively.

absorption for each wavelength, polarization, incident angle, and diffraction order is calculated using its corresponding Fourier coefficients. As an example, this analysis is done for a thin-film silicon slab in the wavelength range between 400 and 1100 nm, for both TM and TE polarizations and under three different angles of incidence. We assess the contribution of both guided and non-guided modes as well as unveil their relative weight with respect to the total absorptance. In this respect, the goal of our work is not just to distinguish between guided and non-guided resonances but to investigate how the absorption seems to be split among the different modes. It should be mentioned that our analysis is limited to planar incidence. Although conical incidence represents the most general case, its study usually leads to anisotropic effects and coupling between s and p polarization, which make the whole analysis more complex.

Without losing generality with respect to our approach,[33] let us consider a 1-μm thick periodically-textured nc-Si:H thin film. The one-dimensional (1-D) texturing has a period of 600 nm, height of 300 nm and duty cycle of 50%. The structure is surrounded by air and it is illuminated with either TE or TM polarized light under oblique incidence θ (see Figure 1).

Figure 1 also shows two scattering events inside the absorber. In region I, light is scattered into many discrete angles by the front surface of the absorber. In region II, a second scattering event is shown, whereby light is scattered once again, this time by the rear surface. In particular, each transmission order from top surface (T_i) re-scatters into all T'_i diffraction orders promoted by the bottom interface. Therefore, a guided mode can couple to other guided modes or to a non-guided mode, and vice versa.[33] In order to distinguish between different resonances inside the absorber, we use Fourier expansion to describe the total electric field inside the absorber, using its Fourier coefficients.[38] This can be done by dividing the grating structure into many thin sub-layers, along the y direction, as depicted in Figure 2(A). The thickness of each sub-layer is defined such that, for the shortest wavelength-in-material ($\lambda = \lambda_0/n$) within the spectral range of interest, there are at least 10 sub-layers within one wavelength. Note that for perpendicular incidence having five sub-layers are sufficient to reach accurate calculation.[33] In oblique angle illumination, however, more sub-layers are needed to reach the same accuracy, especially in the top rim of grating and for TM polarization.

In this way, for each wavelength there are at least 10 sampling points in the material. Within one sub-layer, the electric field is considered to be invariant along the y-axis. At each sub-boundary, the field is expressed using Fourier coefficients. Figure 2(B) shows the x-component of electric field (E_x) at the boundary of 20th sub-layer under 10° illumination and at λ_0 = 730 nm. Since the incident angle is 10°, the electric field inside absorber is not symmetric. Hence, despite the symmetry of the grating, the Fourier coefficients with the same order may not be equal (i.e. $T_{+i} \neq T_{-i}$). This is illustrated in Figure 2(C), where the difference between positive and negative diffraction orders can be clearly observed. For each wavelength, sub-layer and angle of incidence, equation (1) is applied.[33] In this way, for each wavelength and angle of incidence, it is possible to express

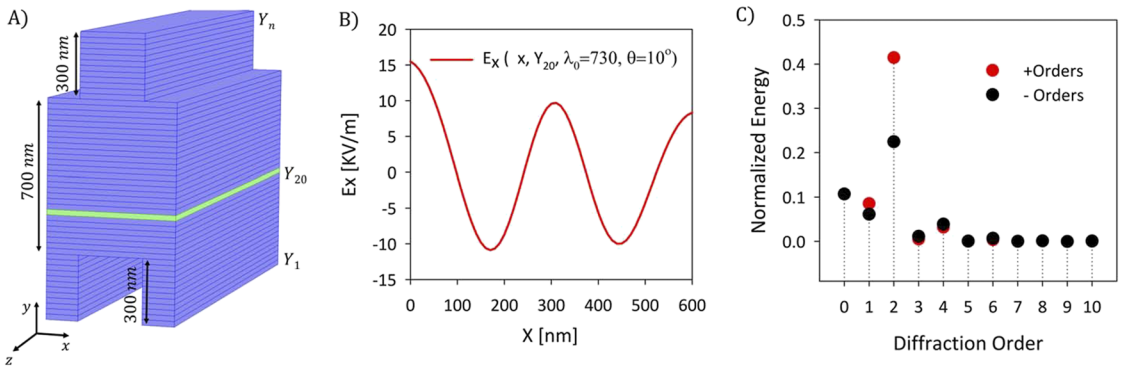

FIG. 2. A) One period of the grating structure, divided into N thin sub-layers with thickness Y_N. B) Intensity of the E_x component of the total electric field in the 20th sub-layer, indicated in green in A), at λ_0 = 730 nm and at 10° angular incidence. C) First 20 orders of the energy spectral density of the electric field, in the 20th sub-layer at λ_0 = 730 nm. Energy is normalized to the total energy in one sub-layer. Since the electric field is asymmetric, efficiency of the positive and negative diffraction orders are not equal.

total absorption as function of the contribution of each diffraction order:

$$\varepsilon_0 nk\omega \int_0^y \int_0^\Lambda |E(x,\lambda_0,\theta_i)|^2 dxdy = \varepsilon_0 nk\omega \sum_{i=y_1}^{i=y_n} \sum_{q=-\infty}^{q=+\infty} \int_0^\Lambda \left|c_{i,q,\lambda_0,\theta_i}\right|^2 dx \quad (1)$$

where ε_0 is the dielectric constant of vacuum, n and κ are real and imaginary parts of the refractive index, respectively, and ω is the angular frequency. $c_{(i,q,\lambda 0,\theta i)}$ is q^{th} Fourier coefficient of the electric field, with wavelengthλ_0, in the i^{th} sub-layer, and for incidence angle θ_i. The left-hand side of equation (1) represents total absorption, while the right-hand side indicates the contribution of each diffraction order, $|c_{i,q,\lambda 0,i}|^2$. In this method, the total electromagnetic field at each point inside the structure needs to be calculated separately, using for example a rigorous electromagnetic simulation tool. This field is then used as an input for equation (1). For our analysis, we employed COMSOL Multiphysics[39] to rigorously calculate the total absorption and total electric field inside the absorber, for both TE and TM polarizations and for three different angles of incidence: 10°, 30° and 60°. Then, the real and imaginary parts of the electric field for each sub-layer, polarization and incidence angle are exported to Mathematica[40] for further analysis. The validation of the method, already demonstrated for perpendicular incidence,[33] is such that total absorption from equation (1) should be equal to the absorption calculated by COMSOL.

The configuration of incidence and diffracted electric field in the grating structure is illustrated in Figure 3. For TE polarized light, the direction of the electric field oscillation does not change inside the absorber. On the other hand, for TM polarized light, the situation is different. The total electric field can be decomposed into E_x and E_y components, whose magnitudes change as function of the incident angle. Figure 3 shows all the components of the electric field inside the absorber, for one particular diffraction angle β. The diffraction angle for each grating order is given by the grating equation: $\beta_q = \sin^{-1}\left(\frac{\sin(\theta_i)}{n} \pm \frac{q.\lambda_0}{n.\Lambda}\right)$, where q is the diffraction order, n is the refractive index, Λ is the grating period, λ_0 is the wavelength *in vacuo* and θ_i is the angle of incidence. In general, for every incident angle θ, more than one diffraction angle is possible. One of the aims of this work is to distinguish between guided and non-guided modes, when the angle of incidence is non-zero ($\theta_i \neq 0$). According to the grating equation, a diffraction order could excite a guided mode resonance only if its diffraction angle is larger than material's critical angle (θ_c) at that wavelength. Therefore, depending on the incident wavelength and angle, a diffraction order could contribute to both guided and non-guided resonances. Total absorption in the grating structure for TE polarized light is calculated by means of equation (1) for three different incident angles, and illustrated in Figure 4. Panels (A), (C) and (E) show absorption for 10°, 30° and 60° angles of incidence, respectively. The oblique incidence implies that $\beta_{+q} \neq \beta_{-q}$. Thus, absorption for the "+qth" and "−qth" orders may not be equal. However, for ease of presentation, total absorption by both "+qth" and "−qth" orders is represented by one color. The nc-Si:H slab can support up to 12 diffraction orders for oblique incident angles, for λ_0 < 450 nm. Nevertheless, for the sake of clarity, Figure 4 only presents the first four diffraction orders. As addressed before, not all diffraction orders can excite a guided mode resonance. For θ_i = 10°, β_{-1} is larger than critical angle (θ_c) when $\lambda \geq$ 496 nm, whereas β_{+1} can excite a guided mode for $\lambda \geq$ 705 nm. For θ_i = 10°, for all higher diffraction orders ($q \leq -2$ and $q \geq 2$), the diffraction angle is larger than the critical angle in the entire wavelength range of interest. Despite the incidence angle, the 0th diffraction order is always a non-guided resonance. Total absorption, due to guided or non-guided resonance for each incident angle, is shown in Figure 4(B), (D) and (F). There, we can observe energy exchange between guided and non-guided resonances. For example, in Figure 4(B) at λ = 795 nm the notch in the blue curve perfectly matches with the peak in red. This is a clear example of energy transfer from non-guided resonance to guided resonance. Additionally, it can be also observed that in TE polarization case total absorption is directly linked to guided resonance absorption. When the incidence angle decreases, the guided resonance absorption decreases significantly and so does the total absorption. It is noteworthy that the method presented in equation (1) is validated for TE polarization, given the excellent superposition of COMSOL- and FFT-computed spectra for all simulated angles of incidence.

TM-polarized light can be described as the superposition of two orthogonally oscillating electric fields, E_x and E_y. E_x represents a plane wave propagating along the $\pm y$ direction. On the other hand, E_y indicates a plane wave propagating along the $\pm x$ direction (parallel to the grating vector). Top and bottom rims of the grating create a non-uniform surface. In other words, depending on x and y coordinates, E_x or E_y can be parallel or perpendicular to the grating surface (locations "a" and "b" in Figure 3). Therefore, under TM-polarized illumination, for any non-zero incident angle, there is a component

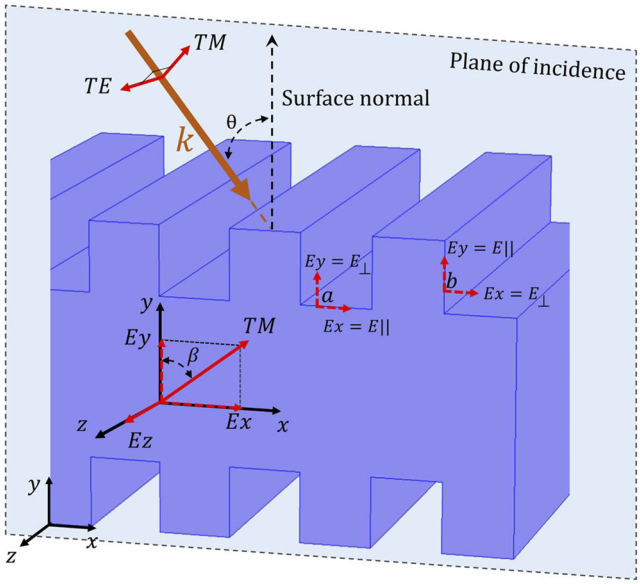

FIG. 3. Configuration of incidence and diffracted electric field for TE and TM polarized light, with incident and diffracted angles θ and β respectively. E_x and E_y components of the electric field in TM polarization vary by changing the incidence angle.

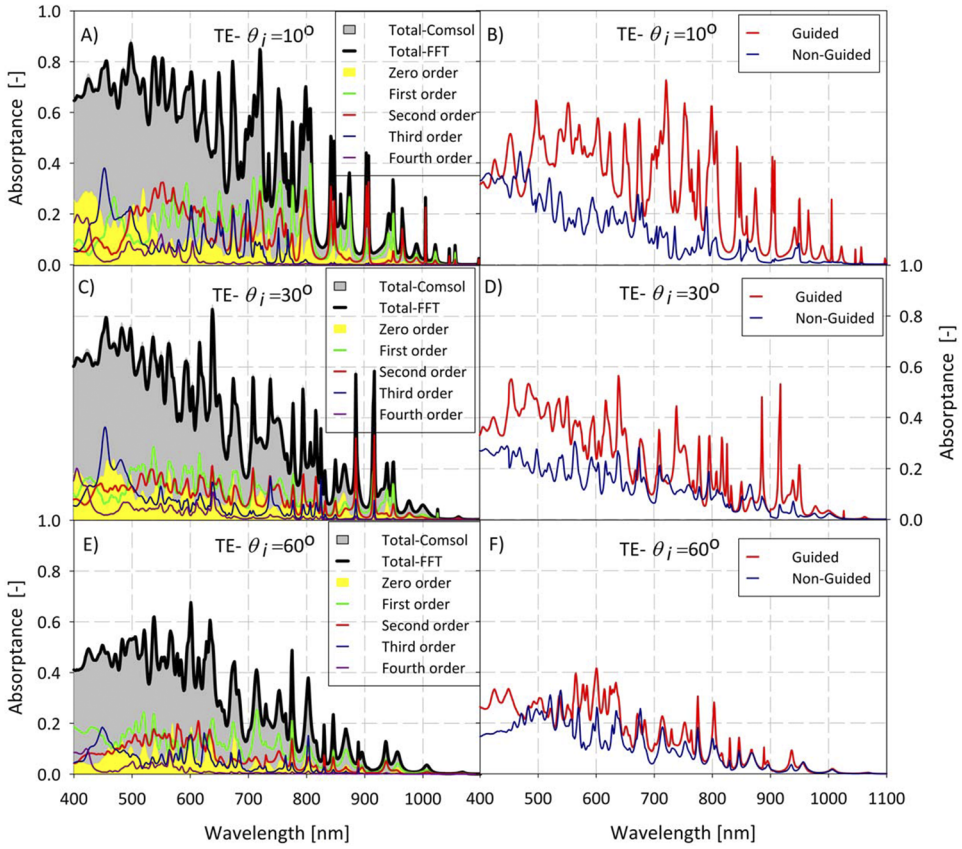

FIG. 4. A), C) and E) Each color represents the absorption in grating structure by TE polarized light for a different diffraction orders and incidence angle. B). D) and F) present the absorptance ascribed to non-guided (blue lines) and guided resonance (red lines), triggered by the absorption of TE polarized light and for different incidence angles.

of the electric field which is perpendicular to the grating surface (i.e. not continuous at the air/nc-Si:H boundary). This discontinuity of the electric field at the interface induces slight error in our calculation using equation (1), mostly located at the short wavelengths. The gap between the grey area and the black line in Figure 5 clearly show this mismatch, which is largest at shorter wavelengths and decreases for larger wavelengths. The reason is that the absorption coefficient of nc-Si:H is very high at short wavelengths, hence almost all incident energy is absorbed by the top rim of the grating (i.e. where the surface is highly non-uniform). Therefore, in this spectral range the discontinuity of the electric field has the maximum influence on our calculations. By decreasing further the thickness of sub-layers (not shown here), this mismatch can be significantly reduced. Each color in Figure 5(A), (C) and (E) represent the absorption for a particular diffraction order, under TM polarized light. In Figure 5, the total TM polarized light, sum of E_x and E_y components, is shown. The contribution of each of those components in total absorption is presented in Figure 6. For the sake of clarity, absorption for the "$+q^{th}$" and "$-q^{th}$" orders are once again plotted together. Interestingly, the result is that in TM polarization case total absorption increases slightly by increasing the angle of incidence. Conversely, guided resonance absorption at shorter wavelengths increases as the incidence angle increases.

As it has been addressed before, TM polarized light can be decomposed into two orthogonally polarized components, E_x and E_y. It is interesting to look at the electric components of TM polarized light, that is, to see how E_x and E_y contribute to the total absorption at each incident angle. Graphs (A), (C), (E) and (B), (D), (F) in Figure 6 show the absorptance under different incident angles for E_x and E_y components, respectively. Each color in Figure 6 shows total absorption for the "+qth" and "$-q^{th}$" orders combined. It is important to notice that absorption for the 0th order diffraction of the E_y component is zero. As it has been addressed before, E_y can be seen as a plane wave propagating along the x-axis. In plane waves, the electric field and propagation vectors are always perpendicular to each other.[41] Therefore, the 0th diffraction order (with propagating vector along y) has $E_y = 0$. For $\theta_i = 10°$, 30° and 60°, all the absorption peaks at $\lambda_0 > 705$, > 905 and > 560 nm are directly connected to the excitation of guided modes, because their diffraction angles are larger than their respective critical angles.

Without the presence of the grating, the structure would be a flat thin film. Such a structure can be seen as a 1-D photonic crystal consisting of only one layer. One of the properties of photonics crystals is their band gap structure. Inside a band-gap, the density of the modes (DOM) is low and thus waves in range of frequencies are forbidden and cannot be transmitted through the material. At the edge of the band gap, however, the DOM is very large[42] and, consequently, the group velocity is very low, meaning that energy travels slowly and therefore the interaction time between light and the film is enhanced. The presence of grating at the film interface breaks the

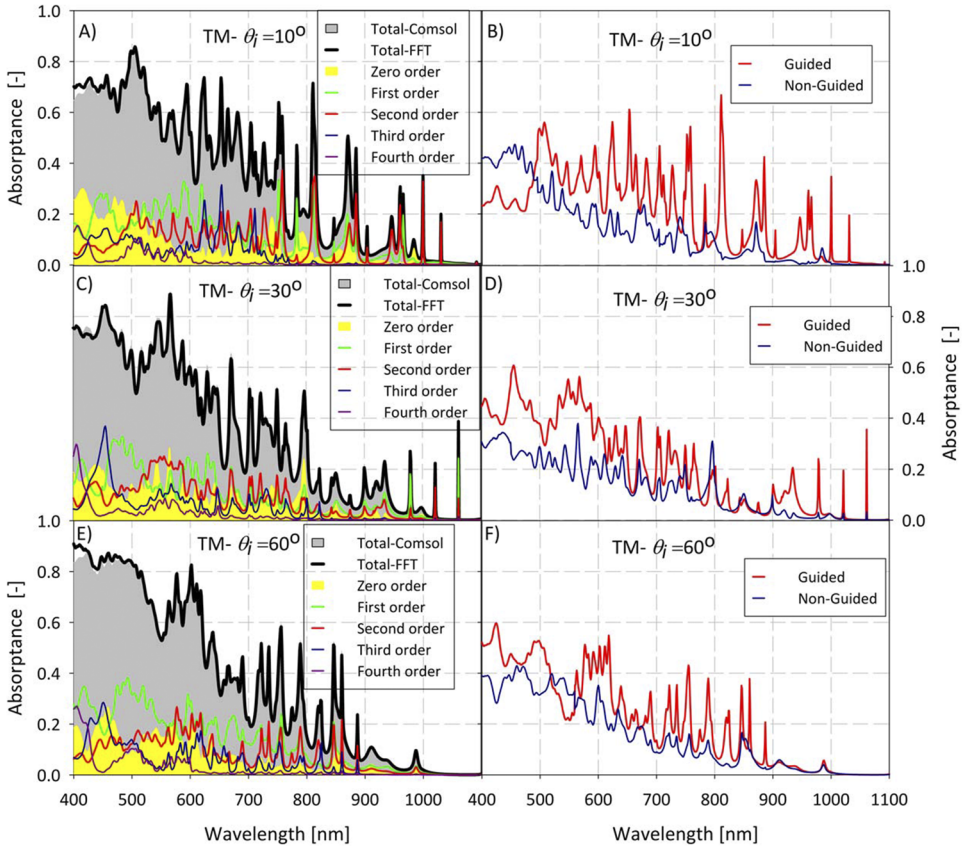

FIG. 5. A), C) and E) show absorption in grating structure for each diffraction order when it is illuminated using TM polarization with 10°, 30° and 60° oblique incidence, respectively. Diagrams B), D) and F) show the contribution on absorptance of guided and non-guided resonances for each incidence angle.

photonics band gap and creates more resonances. A higher number of resonances ultimately indicates a larger DOM which leads to higher absorption.

The DOM in the structure for TE polarized light with 10° incidence angle is presented by gray curve in Figure 7. The DOM for this structure was carried out by computing complex transmission coefficients in COMSOL Multiphysics and then plugging them in Equation 7 of Reference 42. The mode density augments at the photonics band edge. This means that the edge of each absorption peak (absorption by one diffraction order and not the total absorption) should correspond with a peak in DOM. In Figure 7, for sake of visibility, the DOM peaks are re-scaled to one. This information can be used in thin film solar cells design. If the thickness of the thin film is defined, then the band gap of the structure is defined as well. To enhance the absorption, the grating shall be designed in such a way that efficiently excites the modes at the edge of the band gap, where the mode density is higher.

In conclusion, we would like to emphasize that we have employed a Fourier expansion approach to calculate the spectral energy density of the electric field inside a periodically-textured nc-Si:H slab, under oblique incidence and for both TE and TM polarizations for 1D grating. Numerical and rigorous calculations were provided to support our approach. Our proposed method can be used to calculate the absorption for each diffraction order, and to distinguish between guided and non-guided resonances regardless of grating height, incident angle and wavelength range. With the right meshing, it is possible to achieve a very good accuracy even at short wavelengths. This work was triggered by the limitation of intersection method.[43–45] As we describe in our previous work,[33] it is very challenging to track guided modes in a highly textured structure using the dispersion diagram of a flat structure with the same optical thickness as the grating structure. The optical thickness of a grating structure largely depends on the grating properties such as height, duty cycle and grating profile. For a wavelength-scale structure, it is even more challenging to define one optical thickness for all diffraction orders. In the method hereby proposed, tracking of guided modes is possible without knowing the optical thickness or the dispersion diagram. Another reason for this work is that adding texturing to a flat structure might behave as an antireflection layer and thus enhance the absorption by enhancing the light coupling into non-guided resonance rather than guided modes. Our proposed method enables tracking the distribution of incidence energy within different resonances. Although our method is not a grating design tool, it can be used to assess the performance of a new grating design or of an existing one. This is because in our method we rely on the computed electric field *inside* the structure, rather than the grating *profile*. However, this method can be used by grating designers to evaluate the impact of their design on the performance of the entire system, or to better understand how manufacturing errors influence the optical performance of the structure.

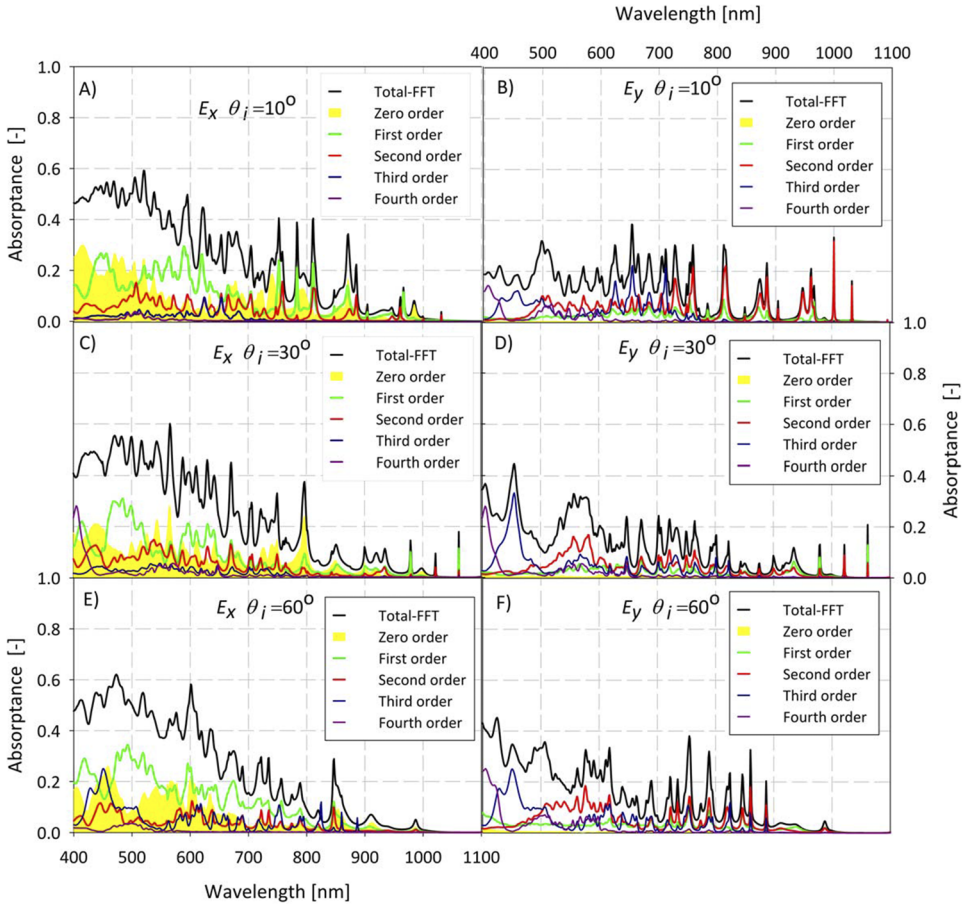

FIG. 6. Panels A), C) and E) show total absorptance spectra for each diffraction order of the E_x component for the three studied incident angles. Total absorptance spectra for each diffraction order of the E_y component for the three studied incident angles are shown in panels B), D) and F).

Another application of our method is to calculate the absorption enhancement (total absorption over one pass absorption) for a particular diffraction order. Since the absorption for each resonance is known, we are able to calculate the absorption enhancement for that resonance without using the Temporal Coupled-Mode Theory (TCMT).[46] Our method can be used for any grating period, wavelength range or incidence angle. However, for grating structures with curved or non-rectangular surfaces, this method probably does not provide accurate result in the non-uniform part of the structure. In this situation, the thickness of sub-layers in the non-uniform part of the structure has to be very thin (depending on the wavelength, grating profile and polarization) to achieve accurate results. In the uniform region, however, this method can be fully trusted. The same principle can be applied for 2D grating structures to evaluate the optical performance of a real solar cell. In this situation, in each sub-layer a 2-D Fourier transform needs to be employed for each component of electric field (E_x, E_y *and* E_z). Our approach is also not limited to solar cell applications and can be used to understand the light behavior in different multilayer structures with periodic texturing.

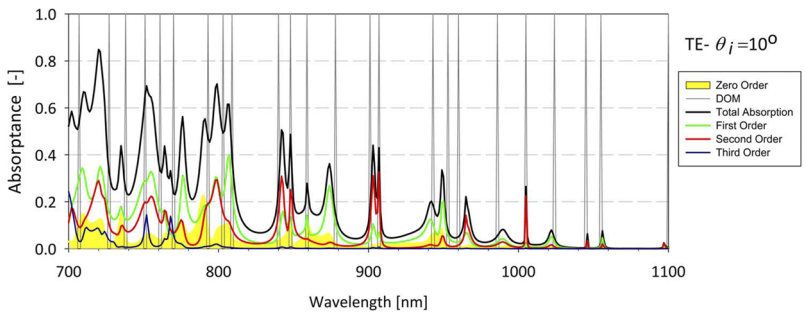

FIG. 7. Density of the modes (DOM) overlaid on the absorptance calculated for the grating structure in case of TE-polarized light with 10° angle of incidence. Most of the peaks in the DOM match with the edge of absorption peaks in the structure.

REFERENCES

[1] C. Gueymard, Solar Energy **76**, 423 (2004).

[2] R. Cariou, J. Benick, F. Feldmann, O. Höhn, H. Hauser, P. Beutel, N. Razek, M. Wimplinger, B. Bläsi, D. Lackner, M. Hermle, G. Siefer, S. W. Glunz, A. W. Bett, and F. Dimroth, Nature Energy **3**, 326 (2018).

[3] F. Sahli, J. Werner, B. A. Kamino, M. Bräuninger, R. Monnard, B. Paviet-Salomon, L. Barraud, L. Ding, J. J. Diaz Leon, D. Sacchetto, G. Cattaneo, M. Despeisse, M. Boccard, S. Nicolay, Q. Jeangros, B. Niesen, and C. Ballif, Nature Materials **17**, 820 (2018).

[4] J. Marko, K. Eike, M.-V. Anna Belen, L. Benjamin, J. Klaus, M. Bart, Al-A. Amran, K. Janez, K. Lars, R. Bernd, S. Rutger, T. Marko, S. Bernd, and A. Steve, Energy Environ. Sci. **11**, 3511 (2018).

[5] D. Grant, K. Catchpole, and K. Weber, Optics Express **24**, A1454 (2016).

[6] K. A. Bush, A. F. Palmstrom, J. Y. Zhengshan, M. Boccard, R. Cheacharoen, J. P. Mailoa, D. P. McMeekin, R. L. Z. Hoye, C. D Bailie, T. Leijtens, I. M. Peters, M. C. Minichetti, N. Rolston, R. Prasanna, S. Sofia, D. Harwood, W. Ma, F. Moghadam, H. J. Snaith, T. Buonassisi, Z. C. Holman, S. F. Bent, and M. D. McGehee, Nature Energy **2**, 17009 (2017).

[7] S. Heping, D. The, P. Jun, J. Daniel, W. Nandi, G. Junbo, W. Yiliang, K. Siva Krishna, F. Xiao, W. Klaus, X. Xudong, W. Thomas P., and C. Kylie, Energy Environ. Sci **11**, 394 (2018).

[8] T. Todorov, O. Gunawan a, and S. Guha, Mol. Syst. Des. Eng. **1**, 370–376 (2016).

[9] B. Yan, G. Yue, L. Sivec, J. Yang, S. Guha, and C. Jiang, Applied Physics Letters **99**, 113512 (2011).

[10] K. Söderström, G. Bugnon, R. Biron, C. Pahud, F. Meillaud, F. J. Haug, and C. Ballif, Journal of Applied Physics **112**, 114503 (2012).

[11] T. Matsui, H. Jia, M. Kondo, K. Mizuno, S. Tsuruga, S. Sakai, and Y. Takeuchi, "Application of microcrystalline $Si_{1-x}Ge_x$ infrared absorbers in triple junction solar cells," *Proceedings of the 35th IEEE Photovoltaic Specialists Conference (PVSC 2010)*, Honolulu, Hawaii, USA, 20-25 June 2010, pp 000311–000316.

[12] J. Bailat, L. Fesquet, J. B. Orhan, Y. Djeridane, B. Wolf, P. Madliger, J. Steinhauser, S. Benagli, D. Borrello, and L. Castens, "Recent developments of high-efficiency micromorph tandem solar cells in KAI-M PECVD reactors," *Proc: 25th European Photovoltaic Solar Energy Conference and Exhibition, 5th World Conference on Photovoltaic Energy Conversion*, Valencia, Spain, 6-10 September 2010, 2720–2723.

[13] H. Sakaki, T. Tanoue, K. Yokoyama, D. C. Sun, Y. Sekiguchi, and Y. Yukimoto, Japanese Journal of Applied Physics **20**, 127 (1981).

[14] A. Barnett, D. Kirkpatrick, C. Honsberg, D. Moore, M. Wanlass, K. Emery, and D. Salzman, Progress in Photovoltaics: Research and Applications **17**, 75 (2009).

[15] S. Kim, F. Takahashi, S. Kasashima, P. Sichanugrist, T. Kobayashi, T. Nakada, and M. Konagai, "Development of thin-film solar cells using solar spectrum splitting technique," in *proceeding of 38th IEEE Photovoltaic Specialists Conference (IEEE, 2012)*, Austin, Texas, USA, June 3-8, 2012, pp 001209–001211.

[16] C. N. Eisler, E. D. Kosten, E. C. Warmann, and H. A. Atwater, "Spectrum splitting photovoltaics: Polyhedral specular reflector design for ultra-high efficiency modules," *39th IEEE Photovoltaic Specialists Conference, (2013)*, Tampa, Florida, June 16-21, 2013.

[17] M. S. Jang and H. Atwater, Physical Review Letters **107**, 207401 (2011).

[18] S. Chetan Singh and S. Hemant Kumar, *Anti-reflection and Light Trapping in c-Si Solar Cells* (Springer, 2017), p 65–82.

[19] T. Söderström, F. J. Haug, X. Niquille, and C. Ballif, Progress in Photovoltaics: Research and Applications **17**, 176 (2009).

[20] H. Sai and M. Kondo, Journal of Applied Physics **105**, 094511 (2009).

[21] H. Iida, N. Shiba, T. Mishuku, H. Karasawa, A. Ito, M. Yamanaka, and Y. Hayashi, IEEE Electron Device Letters **4**, 157 (1983).

[22] F. J. Haug, K. Söderström, A. Naqavi, and C. Ballif, Journal of Applied Physics **109**, 084516 (2011).

[23] G. Yue, L. Sivec, J. M. Owens, B. Yan, J. Yang, and S. Guha, Applied Physics Letters **95**, 263501 (2009).

[24] K. Söderström, J. Escarré, O. Cubero, F. J. Haug, S. Perregaux, and C. Ballif, Progress in Photovoltaics: Research and Applications **19**, 202 (2011).

[25] B. Lipovšek, J. Krč, O. Isabella, M. Zeman, and M. Topič, Journal of Applied Physics **108**, 103115 (2010).

[26] O. Isabella, S. Dobrovolskiy, G. Kroon, and M. Zeman, Journal of Non-Crystalline Solids **358**, 2295 (2012).

[27] T. Koida, H. Fujiwara, and M. Kondo, Applied Physics Express **1**, 041501 (2008).

[28] Z. Yu, A. Raman, and S. Fan, Proceedings of the National Academy of Sciences of the United States of America **107**, 17491 (2010).

[29] O. Isabella, R. Vismara, D. N. P. Linssen, K. X. Wang, S. Fan, and M. Zeman, Solar Energy **162**, 344 (2018).

[30] N. Rezaei, O. Isabella, Z. Vroon, and M. Zeman, Solar Energy **177**, 59 (2019).

[31] H. Savin, P. Repo, G. von Gastrow, P. Ortega, E. Calle, M. Garín, and R. Alcubilla, Nature Nanotechnology **10**, 624 (2015).

[32] D. Freier, R. Ramirez-Iniguez, T. Jafry, F. Muhammad-Sukki, and C. Gamio, Renewable and Sustainable Energy Reviews **90**, 957 (2018).

[33] H. Ahmadpanahi, R. Vismara, O. Isabella, and M. Zeman, Opt. Express **26**, A737 (2018).

[34] S. A. Shakir and A. F. Turner, Appl. Phys. A **29**, 151 (1982).

[35] F.-J. Haug, K. Söderström, A. Naqavi, C. Battaglia, and C. Ballif, MRS Proceedings **1391**, 11 (2012).

[36] O. El Gawhary, N. J. Schilder, A. da Costa Assafrao, S. F. Pereira, and H. P. Urbach, New Journal of Physics **14**, 053025 (2012).

[37] O. El Gawhary, M. C. Dheur, S. F. Pereira, and J. J. M. Braat, Appl. Phys. B **111**, 637 (2013).

[38] R. Bracewell, *The Fourier Transform and Its Applications* (Mcgraw-Hill, 3th Edition), p. 120.

[39] See: https://www.comsol.eu/ For more information about COMSOL Multiphysics; Last access 17 October 2018.

[40] For more information about Wolfram Mathematica please visit: http://www.wolfram.com/mathematica/ (last access 17 October 2018).

[41] J. A. Stratton, *Electromagnetic Theory* (John Wiley & Sons, Inc, (2015), p. 83–159.

[42] J. M. Bendickson, J. P. Dowling, and M. Scalora, Phys. Rev. E **53**, 4107 (1996).

[43] A. Naqavi, F. Haug, H. P. Herzig, and C. Ballif, in *Renewable Energy and the Environment Optics and Photonics Congress, OSA Technical Digest (online)* (Optical Society of America, 2012), Eindhoven, Netherlands, 11–14 November 2012, paper JM5A.21.

[44] K. Söderström, PhD thesis, École polytechnique fédérale de Lausanne, STI, Lausanne, 2013.

[45] F. J. Haug, T. Söderström, O. Cubero, V. Terrazzoni-Daudrix, and C. Ballif, Journal of Applied Physics **106**, 044502 (2009).

[46] Z. Yu, A. Raman, and S. Fan, Optics Express **18**, A366 (2010).